Magnetoelectronic properties of a ferrimagnetic semiconductor: The hybrid cupromanganite $CaCu_3Mn_4O_{12}$

Ruben Weht[1] and Warren E. Pickett[2]

[1]*Departamento de Física, CNEA, Avda. General Paz y Constituyentes, 1650, San Martín, Argentina*
[2]*Department of Physics, University of California, Davis, California 95616*

The mixed manganite cuprate $CaCu_3Mn_4O_{12}$ is calculated, using density functional methods, to be a spin-asymmetric ferrimagnetic semiconductor with a small gap. Cu (formally spin $\frac{1}{2}$) antialigns with Mn (formally spin $\frac{3}{2}$), and the net spin moment is $9\mu_B$, consistent with the formal spins. The valence-band maximum has Cu d_{xy}–O p_σ character with spin aligned antiparallel with the net magnetization; the conduction-band minimum has the opposite spin and mixed Cu-Mn character. This spin-asymmetric gap (1) implies a thermally induced current that is 100% spin polarized and (2) leads to a field-induced narrowing of the energy gap. The relationship of these properties to the reported magnetoresistance is discussed.

I. INTRODUCTION

Reports in the past few years of very high values of the magnetoresistance (MR) in manganite perovskites have stimulated a tremendous interest in those compounds,[1] already known from seminal works in the 1950s. These manganites, now called colossal magnetoresistance (CMR) materials, are attracting a level of attention only rivaled by the continued interest in the high-temperature cuprates, which are based on a related transition-metal oxide structure. With the development of more and more complex materials by both conventional growth techniques and artificial, nonequilibrium growth procedures, it was inevitable that the combination of Cu and Mn oxides would be explored.

The attractiveness of studying these systems comes, on the one hand, because of new properties and possible applications and, on the other, from the richness of their very complex phase diagrams that in both cases may be viewed from an undoped antiferromagnetic (AFM) insulator (I) parent compound. In manganites, viz., $La_{1-x}Ca_xMnO_3$, the phase diagram shows strong competition between lattice, spin, charge, and orbital degrees of freedom. Coming from the La-rich end, the AFM-I phase gives way to a ferromagnetic (FM) metal (M), while from the Ca-rich side the system remains insulating down to $x=0.50$ while displaying a variety of charge, spin, and orbitally ordered phases. In layered cuprates the AFM-I phase gives way to a metallic phase that becomes superconducting at remarkably high temperatures, over 100 K in several cases.

The high values of MR observed in the manganites suggest applications as new magnetoelectronic devices. However, before widespread practical uses can be made, some of their properties have to be improved. In particular, there are two limiting factors in their performance: one is that the highest values of MR can be reached only below room temperature and at high magnetic fields (below 250 K and several tesla for $La_{3/4}Ca_{1/4}MnO_3$). Moreover, their MR is large only in a very narrow temperature interval near the insulator-metal and the paramagnetic-ferromagnetic transitions.

Both from the point of view of the manganite-cuprate combination and for the possibility of improving device characteristics, the recent report by Zeng *et al.*[2] constitutes an intriguing new development. This group has shown that the hybrid cupromanganite $CaCu_3Mn_4O_{12}$ (CCMO), which is an ordered perovskite with quadrupled primitive unit cell, presents a quite large MR (up to several tens of percent) at relatively low magnetic fields without the presence of either a mixed valency or metal-insulator transition. Moreover, this colossal MR extends over a wide temperature range.

This compound contains two magnetic ions, formally given as Mn^{4+} ($d^3, S=\frac{3}{2}$) and Cu^{2+} ($d^9, S=\frac{1}{2}$), on two crystallographically distinct sites. Both its resistivity $\rho(T)$ and magnetization $M(T)$, measured on polycrystalline samples, show unconventional behavior. $\rho(T)$ is semiconducting in magnitude and also in temperature derivative, but has *no* visible anomaly at the Curie temperature $T_C=355$ K. $M(T)$, on the other hand, shows a steep, nearly first-order-like jump at T_C to $\sim 80\%$ of its saturation value. The temperature dependence of the activated resistivity (over a limited temperature range) suggests an energy gap of ~ 0.12 eV.

The basic electronic, and even magnetic, structures of this compound are not established. In this work we present the electronic and magnetic characteristics of this material and relate them to its transport and magnetic properties. In Sec. II we describe the distorted quadruple perovskite structure and outline our method of calculation. The results for the band structure, density of states, and magnetism are given in Sec. III. In Sec. IV we discuss the avenues for magnetic coupling in CCMO. The relation of our results to the measured $\rho(T)$ and MR is discussed in Sec. V.

II. CRYSTAL STRUCTURE AND METHOD OF CALCULATION

A. Structure

The crystal structure, shown in Fig. 1 and discussed in detail by Chenavas *et al.* 25 years ago,[3] is a strongly distorted ordered version of a perovskite with formula $Ca_{1/4}Cu_{3/4}MnO_3$. Formal valence ideas suggest a Cu^{2+} ion,
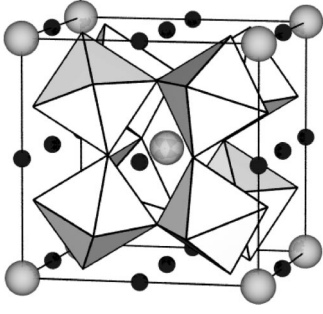
FIG. 1. The crystal structure of the quadruple-perovskite compound $CaCu_3Mn_4O_{12}$. Two primitive cells of the bcc structure are shown. Oxygen atoms lie at the vertices of the octahedra; Mn lies at their centers. The large (small) spheres represent Ca (Cu).

so the system is isovalent with $CaMnO_3$ and hence expected to be insulating, as observed. Here the Cu^{2+}, but not the Mn^{4+}, ion is expected to be a Jahn-Teller ion, leading to an oxygen sublattice that corresponds to a tilted three-dimensional network of MnO_6 octahedra. The Mn-O-Mn angle becomes $\approx 142°$ instead of $180°$, as in the ideal perovskite structure. Two types of polyhedra are present at the A position: a just slightly distorted O icosahedron around the Ca site and a roughly square planar O-coordinated Cu site with a Cu-O distance of 1.94 Å. The quadrupled perovskite cell has space group $Im3$ ($\equiv I2/m\bar{3}$, No. 204 in the International Tables).

The quadrupling and distortion of the perovskite structure leads to low site symmetries. The cations nevertheless all sit on the usual ideal positions of the cubic perovskite lattice. The symmetry lowering arises from the replacement of 75% of the Ca (in $CaMnO_3$) by Cu and by rotation of the O octahedra which leaves O sites of the form $(0,y,z)$ ($y = 0.3033, z = 0.1822$) and only mirror site symmetry. The Mn site at $(\frac{1}{4},\frac{1}{4},\frac{1}{4})a$ has $\bar{3}$ symmetry, because each MnO_6 octahedron rotates to retain a triangular face perpendicular to a $\langle 111 \rangle$ direction. The Cu site has mmm symmetry, while the Ca site is in a $m3$ position. The lattice constant a is approximately twice the related simple perovskite cell, and the Bravais lattice is bcc.

This structure is closely related to that of the skutterudite, $CoSb_3$.[4] Both are members of a class that can be generally denoted as $A'A_3''T_4B_{12}$, where A' and A'' are cations, T is a metal (usually transition metal) ion, and B is an anion. The underlying structure is perovskite. The relation of $CoSb_3$ to the $CaCu_3Mn_4O_{12}$ structure is Co→Mn; Sb→O; the Sb_4 square becomes the CuO_4 square; the Ca ion fills the La site in filled skutterudites (like $LaCo_4Sb_{12}$). In skutterudites there is no counterpart of the Cu ion in $CaCu_3Mn_4O_{12}$.

It should be noted for the analysis that follows that the CuO_4 "square" is in fact not actually a square although all Cu-O bond lengths are equal. Rather it is a rectangle whose O-Cu-O angles are $85.6°$ and $94.4°$. As a result the Cu d_{xy}, d_{yz}, and d_{zx} orbitals are not related by symmetry. In particular, we will use the term "CuO_4 square," and when we discuss it, we will have in mind a local coordinate system in which the square lies in the x-y plane.

In the same way the Mn d orbitals cannot be exactly associated with the standard t_{2g}/e_g symmetries. Instead, the $\bar{3}$ symmetry of Mn dictates that, in the local coordinate system where the threefold axis is the $\hat{z}$ axis, the irreducible representations of the five $3d$ states are $3z^2-r^2, \{xz,yz\}$, and $\{xy,x^2-y^2\}$. This $3z^2-r^2$ state is a symmetric linear combination of the three t_{2g} orbitals in the usual frame of the MnO_6 octahedron.

B. Calculations

We have applied the linearized augmented plane-wave (LAPW) method,[5] which utilizes a fully general shape for density and potential. The WIEN97 code[6] has been used in the calculations. The experimental lattice constant of 7.241 Å was used. LAPW sphere radii (R) of 1.90 a.u. were chosen for the Cu and Mn atoms, 2.00 a.u. for Ca and 1.60 a.u for O, with cutoffs of RK_{max} up to 7.0, providing basis sets with more than 1800 functions per primitive cell. Self-consistency was carried out on k points meshes of up to 60 points in the irreducible Brillouin zone (BZ) (1000 points in the complete BZ). The generalized gradient approximation (GGA) exchange-correlation functional of Perdew *et al.*[7] was used in the present work.

A previous study of the electronic structure of CCMO has been reported by Wu, Zheng, and Gong[8] using a local combination of atomic orbitals method. Using the local spin density approximation (LSDA) they did not obtain a gap as seen in experiment, so they turned to the LSDA+U method.[9] This method is known to separate the occupied and unoccupied states of the atom(s) the repulsive potential U is applied to, and it was expected to, and did, produce a gap. One result of our work is that the GGA exchange-correlation functional, applied within the more accurate LAPW method, produces a gap and gives properties in reasonable agreement with experiment, so there is no reason to turn to *ad hoc* methods.

Moreover, application of the LDA+U method to a complex compound such as CCMO is more problematic than usual. To apply the modern form, one requires four parameters: the screened Coulomb repulsion U and the screened exchange J for both Cu and Mn. The parameters are system dependent and their variation with their environment is not understood. To apply LDA+U systematically would require a separate concerted effort.

III. COMPUTATIONAL RESULTS

A. Band structure

The majority and minority band structures bounding the gap are shown in Fig. 2, and the corresponding densities of states (DOS) in Fig. 3. The calculated gaps are 0.50 eV for spin up (parallel to the net magnetization) and of 0.18 eV for spin down, both direct. For the minority carriers the gap occurs at H between pure Cu d_{xy} states below the gap to Mn t_{2g} character above. The thermal gap is quite small, 0.09 eV, and *indirect* between the spin down valence-band maximum at H and the spin-up conduction-band minimum at Γ. It is common for the band gap in density functional calculations to be smaller than the true gap, but the band character and
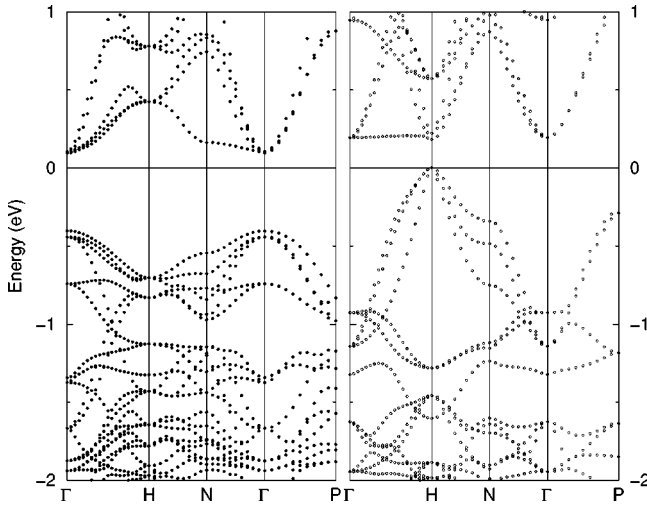
FIG. 2. Band structures near the energy gap for spins up (left panel) and down (right panel). Note the spin-asymmetric character: the valence-band maximum occurs for spin down (right panel), the conduction-band minimum occurs for spin up (left panel). $\Gamma = (0,0,0)$, $H = 2\pi/a$ (1, 0, 0), $N = (2\pi/a)(\frac{1}{2},\frac{1}{2},0)$, and $P = (2\pi/a)(\frac{1}{2},\frac{1}{2},\frac{1}{2})$.

shape on either side of the gap are nonetheless given reasonably. In this case the calculated gap is quite similar to the experimental estimate.

The bands at the valence-band maximum (spin down) have a strong Cu d character. They are the result of the $dp\sigma$
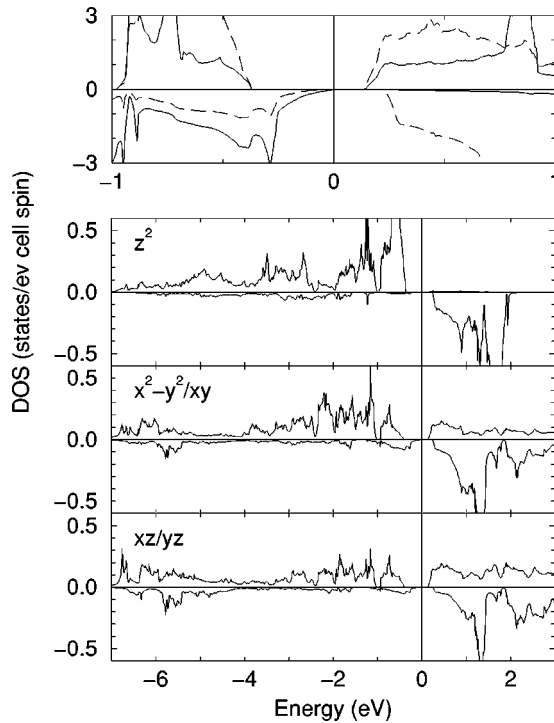

FIG. 3. Bottom: partial density of states for the Mn atom, decomposed according to the local frame symmetries. Top: a detail of the partial density of states around the gap, with Cu as the solid line and Mn as the dashed line. The zero of energy lies within the gap.
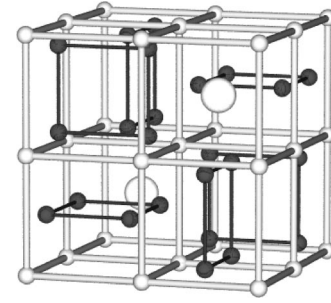

FIG. 4. A skeleton drawing of the $CaCu_3Mn_4O_{12}$ structure, emphasizing the CuO_4 "squares." Small gray dots represent the Mn ions, while the squares represent the CuO_4 units with black O ions. The Cu ion lies at the center of the square and is not shown. The large light gray sphere denotes Ca. This figure is displaced by $(a/4,a/4,a/4)$ from the regions shown in Fig. 1.

antibonding interaction of the d_{xy} with O p_σ orbitals in the CuO_4 square and are the analog of the $d_{x^2-y^2}$ states in the layered cuprates.

This bonding makes a band with a dispersion of almost 1.5 eV. We will denote the $dp\sigma$ antibonding combination of the Cu d_{xy} and the four neighboring O $p\sigma$ orbitals as $\mathcal{D}_{xy}$. The other Cu d orbitals are concentrated in a small region between 1 and 2.5 eV below the gap.

If the CuO_4 unit were actually a square, $\mathcal{D}_{xy}$ would not couple with other Cu d–O p combinations. However, since this is not exactly true, the Cu d_{xy} orbital will also mix with inplane O p_π orbitals via $dp\pi$ coupling, which may not be negligible.

From the depiction of the CuO_4 squares in Fig. 4, it can be seen that the $\mathcal{D}_{xy}$ functions on neighboring squares are orthogonal by symmetry. As a result, the dispersion, which is 1.2 eV along H-Γ, cannot develop from direct $\mathcal{D}_{xy}$-$\mathcal{D}_{xy}$ hopping.

The symmetry character of the Mn d shell is important to identify, since it affects the magnetic coupling. As expected for the Mn^{4+} (d^3) ion the corresponding t_{2g} and e_g orbitals [in the usual octahedron-adapted coordinates, in which the axes extend from Mn through the neighboring O ions (or nearly so)] are well separated, with the t_{2g} majority orbitals filled: a fully polarized d^3 configuration.

While this picture is certainly roughly true, there is another important and precise aspect to the exact site symmetry of Mn. The Mn d DOS, decomposed into the local symmetry-adapted frame, indicates that it is the z^2 state alone (along the threefold axis) that is completely occupied in the majority bands and very nearly completely unoccupied in the minority bands. The other two twofold irreducible representations are strongly mixed in both the majority occupied and unoccupied states.

B. Magnetic structure

The calculations were initiated with magnetic Cu and Mn ions aligned in ferromagnetic fashion. Both Mn and Cu ions remain magnetic, but the Cu moments strongly favor being *antiparallel* to the Mn moments, resulting in a ferrimagnetic spin ordering. The resulting moments inside the muffin tin

spheres are $2.42\mu_B$ and $-0.45\mu_B$ for Mn and Cu, respectively, compared to the ideal values ($S=\frac{3}{2}$, $3\ \mu_B$ for Mn and $S=\frac{1}{2}$, $1\mu_B$ for Cu). This reduction results from hybridization with the O $2p$ states, as observed in other transition-metal oxides. The net magnetic moment is $9\mu_B$ per formula unit, which is also what would be obtained from the formal moments aligned ferrimagnetically. The magnetic moment on the Cu ion is a result of the exchange splitting of the $\mathcal{D}_{xy}$ orbital, which in this coordinate system is the orbital with lobes pointing to the nearest-neighbor oxygens. The almost electronically isolated CuO square favors this configuration as was shown previously in other zero- or one-dimensional copper oxides.[10,11] Magnetism in the Mn ion comes as expected from the splitting of the t_{2g} orbitals and filling only of the spin up states.

From this point of view, our results offer a different interpretation for the nature of the semiconducting behavior of this material respect to the previous LDA+U report.[8] Using the GGA exchange-correlation functional and the LAPW method, $CaCu_3Mn_4O_{12}$ is predicted to be a small gap semiconductor. Determining whether stronger correlation corrections are necessary to describe $CaCu_3Mn_4O_{12}$ properly will require more experimental data.

An experimental study of the magnetic arrangements in $CaCu_3Mn_4O_{12}$ has been reported. Since Cu and Mn have x-ray scattering strengths that are similar, neutron scattering has been used and has established that some samples are nonstoichiometric, with the (also Jahn-Teller active) Mn^{3+} ion substituting partially on the Cu site.[12] In these samples the order may be ferromagnetic or canted. In a nearly stoichiometric sample, the total magnetization decreased and the conclusion was that ferrimagnetic ordering was likely.

To investigate how strong this ferrimagnetic configuration is, we have done fixed spin moment calculations. If the Mn^{4+} spin ($3\mu_B$) is aligned with the Cu^{2+} spin ($1\mu_B$), the total moment is $15\mu_B$. Fixing the total moment at this value, we obtain a highly unstable state almost 1 eV higher in energy than for ferrimagnetic alignment, with some changes of the individual magnetic moments. Supposing a near-neighbor spin Hamiltonian with a Cu-Mn coupling of the form

$$H^{Cu\text{-}Mn}=\sum_{\langle ij\rangle}J_{ij}^{Cu\text{-}Mn}\hat{S}_i^{Cu}\cdot\hat{S}_j^{Mn}, \qquad (1)$$

with the sum being over pairs and with spin vectors normalized to unity, the three Cu ions per cell and eight Mn neighbors per Cu would lead to an energy difference of $2J\times 8\times 3=48J\approx 1$ eV, giving an AFM exchange coupling of $J^{Cu\text{-}Mn}\approx 21$ meV.

The magnetism of $CaCu_3Mn_4O_{12}$ presents several interesting questions. First of all, the exchange splitting of the Cu d_{xy} state is $\Delta_{ex}^{Cu}\sim 1.2$ eV. This value can be understood from the DOS shown at the top of Fig. 3. Although such exchange splittings are less apparent in ferrimagnets than in simple ferromagnets, this Cu d orbital is separate from the other Cu d orbitals (at higher energy), making it possible to identify the splitting. Given its moment of $m_{Cu}=0.45\mu_B$ (inside its muffin tin sphere), there results a ratio Δ_{xy}^{Cu}/m_{Cu}

$=2.7$ eV/μ_B; a very large value considering this ratio (the Stoner I_{xy}^{Cu} in the relation $\Delta_{ex}=Im$) is usually no more than 1 eV/μ_B in transition-metal magnets. The exchange splitting of the other Cu d orbitals is smaller, of the order of 0.4 eV. This difference reflects a strongly anisotropic exchange potential on the Cu ion, which may be due in large part to the ferrimagnetic order.

The exchange splitting on the Mn ion is harder to estimate, due to the strong dissimilarity of the majority and minority d DOS [Fig. 3(a)]. This is a rather common occurrence in ferrimagnets, where the spin-up bands cannot be regarded as an exchange-shifted version of the spin-down bands, even to zeroth order. Complications due to the ferrimagnetism may also be the cause of the surprisingly large value of I_{xy}^{Cu}.

IV. MAGNETIC COUPLING

The magnetic coupling in $CaCu_3Mn_4O_{12}$ is potentially quite complex to unravel due to the two types of magnetic ions and the large cell with low-symmetry sites.[3,13] The bond angles involved in the various exchange processes in $CaCu_3Mn_4O_{12}$ are O-Cu-O, 85.6° and 94.4°; O-Mn-O, 90.0°; Mn-O-Mn, 142°; Cu-O-Mn, 108.7°. Nearest neighbor bond distances are d(Mn-O)$=1.915$ Å, d(Cu-O) $=1.942$ Å, and d(Ca-O)$=2.56$ Å. Note that in the undistorted structure with 12-fold-coordinated Cu, d(Cu-O) would be $\sqrt{2}a/4=2.56$ Å; i.e., the rotation of the MnO$_6$ octahedra decreases the Cu-O distance by 0.62 Å.

Lacroix[14] has discussed the couplings in the isostructural compound $CaCu_3Ti_4O_{12}$, where Ti is d^0 and therefore there are only Cu-Cu couplings. The observed magnetic order is antiferromagnetic,[15] but with a three-sublattice, noncollinear structure in which three Cu spins in a (111) plane have projections on that plane that lie at 120° angles to each other. The three Cu spins in the next (111) layer are antiparallel to the first three. Lacroix argues that, because the exchange coupling path is through the TiO$_6$ octahedron, first-, second-, and third-neighbor Cu-Cu coupling $J_m^{Cu\text{-}Cu}$ ($m=1,2,3$) may be comparable in magnitude. This should be true if direct O-O hopping is neglected. Noncollinearity of the spins was attributed to spin-orbit coupling. In $CaCu_3Mn_4O_{12}$ the Cu-Cu geometry is the same, so all three couplings should again be considered. However, the MnO$_6$ octahedron, with its different availabilities of spin-up and spin-down Mn d orbitals for the exchange processes, will provide different coupling than would the TiO$_6$ tetrahedron.

In addition, Mn-Mn coupling is essential as well as the Mn-Cu coupling discussed in the previous section. Since Mn spins lie on a simple cubic lattice connected by a single O^{2-} ion, the Goodenough-Kanamori-Anderson (GKA) rules can be applied to understand $J^{Mn\text{-}Mn}$. Further Mn-Mn couplings should be small and not affect qualitative behavior. Whereas 180° Mn^{4+}-O-Mn^{4+} coupling is antiferromagnetic (viz., CaMnO$_3$), when this angle is reduced to 142° a ferromagnetic sign is expected. Parallel alignment of the Mn spins is observed and is the only situation we have considered in our calculations.

Finally, there is the question of the origin of the AFM Mn-Cu coupling. In this structure all oxygen ions are equiva-

lent and each one is coordinated with two Mn ions and one Cu ion. We assume that only a single Mn-Cu coupling is important; this coupling connects a Cu spin to eight Mn neighbors and each Mn spin to six neighboring Cu spins. The ferromagnetic-ferrimagnetic difference in energy in the last section identified $J^{Mn-Cu} \approx 20$ meV (antiferromagnetic).

V. DISCUSSION

The picture we obtain leads to a ferrimagnetic semiconductor with an indirect gap of 90 meV, with valence and conduction bands of oppositely directed spins (down and up, respectively, with respect to the net macroscopic magnetization $\vec{M}$). Here we consider the experimental data of Zeng *et al.* in the light of our predicted electronic and magnetic structure.

Zeng *et al.* interpreted their data in the neighborhood of T_C in terms of a gap of around 120 meV. However, one should note that their measured resistivity does not behave in activated fashion; rather, in the range 25–300 K the resistivity of their sample can be described by the form

$$\rho(T) = \rho_0 e^{-T/T_0}, \quad \rho_0 = 10^5 \ \Omega \ \text{cm}, \quad T_0 = 180 \ \text{K}. \quad (2)$$

Below 25 K, ρ deviates only slightly (upward) from this form. Since these data are from polycrystalline samples, $\rho(T)$ may be affected strongly by extrinsic factors, and the data give only a weak upper bound on the intrinsic resistivity.

Now we consider resistivity and magnetoresistance in the context of the band structure described above.

(1) *Intrinsic field dependence of the carrier concentration.* In a stoichiometric single-magnetic-domain sample of $CaCu_3Mn_4O_{12}$ in zero field, an equal number of electron and hole carriers fixes the position of the chemical potential within the gap, and there will be no spin scattering due to the absence of available spin-flipped states for each type of carrier. An applied field produces a relative shift of the up and down bands by $\frac{1}{2}(g_v + g_c)\mu_B B$, where g_v and g_c are the valence- and conduction-band g factors. If $\vec{B}$ is applied parallel to $\vec{M}$, the gap is narrowed and the carrier density (equal for electrons and holes) increases. The change in the carrier density follows the form

$$\left| \frac{d \log n}{dB} \right| = \frac{1}{2} \bar{g} \frac{\mu_B}{k_B T}, \quad (3)$$

where $\bar{g}$ is the average of the electron and hole g factors. Even if the measured $\rho(T)$ is not intrinsic, as long as it is proportional to the number of excited carriers, the MR may be related to the change in the number of carriers due to the above-mentioned shift in gap due to the applied field. For a gap of 100 meV, the last fraction on the right-hand side for $B = 6$ T (the highest field measured) is 0.16 for $T = 25$ K and 0.013 for $T = 300$ K. If $\bar{g} \sim 2$, the fractional change in carrier density is 17% and 1.3%, respectively. The reported (negative) MR at 5 T was reported to be 35% and 6%–7%, respectively. Since at $B = 5$ T the magnetization will surely

be aligned with the field, the predicted decrease in gap and increase in carrier density with field is comparable to the observed MR.

(2) *Tunneling magnetoresistance.* For granular samples, however, there is another — perhaps more important — effect of the field and one that is independent of the size of the gap. Without a field (and vanishing net magnetization of a multidomain sample) one can assume that neighboring grains i and j have relative directions of their moments (θ_{ij}) distributed randomly, with the tunneling of electrons and holes separately across grain boundaries being proportional to $\cos(\theta_{ij}/2)$. Due to the full polarization, conduction vanishes if the moments of neighboring grains are antialigned, as is the case in half metallic ferromagnets.[16] In the high-field limit, on the other hand, the moments of all grains are aligned: $\cos(\theta_{ij}/2) = 1$. Supposing as usual that the intergrain conductivity is $\sigma_{ij} \propto \cos(\theta_{ij}/2)$, and performing the angular average for the zero-field case, one obtains for high-field MR

$$\lim_{H \to \infty} \frac{\rho(H) - \rho(0)}{\rho(0)} = \frac{0.64 - 1}{1} = -0.36. \quad (4)$$

This value is quite close to the low-temperature, $H = 5$ T result reported by Zeng *et al.* This intergrain MR has the same origin as that discussed for the half metallic ferromagnets CrO_2 (Ref. 17) and Sr_2FeReO_6 (Ref. 18). Note that this intergrain tunneling mechanism does not require undoped material; it only requires fully polarized carriers, which occurs in our picture of $CaCu_3Mn_4O_{12}$ (with both electrons and holes polarized) and in half metallic ferromagnets.

(3) *Unusual contribution to the susceptibility.* There is another novel effect in a spin-asymmetric semiconductor such as we propose $CaCu_3Mn_4O_{12}$ to be. As electrons and holes are thermally excited, not only are each 100% polarized, but they contribute together to a net spin polarization due to the charge carriers. This can be seen by noting that an electron in the valence bands must have its spin flipped to be excited into the conduction band. In $CaCu_3Mn_4O_{12}$, application of a field parallel to the net moment increases the magnetization by the polarization of the carriers. Note that if the asymmetry of the gap were reversed, application of a field parallel to the moment would *decrease* the magnetization; i.e., the carrier susceptibility would be diamagnetic.

[1] R. von Helmolt *et al.*, Phys. Rev. Lett. **71**, 2331 (1993); S. Jin *et al.*, Science **264**, 413 (1994).

[2] Z. Zeng, M. Greenblatt, M.A. Subramanian, and M. Croft, Phys. Rev. Lett. **82**, 3164 (1999).

[3] J. Chenavas, J.C. Joubert, M. Marezio, and B. Bochu, J. Solid State Chem. **14**, 25 (1975); J.C. Joubert *et al.*, in *Ferrites*, Proceedings of ICF3, Third International Conference on Ferrites, Kyoto, 1980 (Reidel, Dordrecht, Netherlands, 1982), p. 400–405.

[4] See the discussion and references in D.J. Singh and W.E. Pickett, Phys. Rev. B **50**, 11 235 (1994); and the figure in B.C. Sales *et al.*, *ibid.* **56**, 15 081 (1997).

[5] D.J. Singh, *Planewaves, Pseudopotentials, and the LAPW Method* (Kluwer Academic, Boston, 1994).

[6] P. Blaha, K. Schwarz, and J. Luitz, computer code WIEN97, Vienna University of Technology, 1997. Improved and updated version of the original copyrighted WIEN code; which was published by P. Blaha, K. Schwarz, P. Sorantin, and S.B. Trickey, Comput. Phys. Commun. **59**, 399 (1990).

[7] J.P. Perdew *et al.*, Phys. Rev. B **46**, 6671 (1992); J.P. Perdew, K. Burke, and M. Ernzerhof, Phys. Rev. Lett. **77**, 3865 (1996).

[8] H. Wu, Q.-Q. Zheng, and X.-G. Gong, Phys. Rev. B **61**, 5217 (2000).

[9] A.I. Liechtenstein, V.I. Anisimov, and J. Zaanen, Phys. Rev. B **52**, R5467 (1995); I. Anisimov, F. Aryasetiawan, and A.I. Liechtenstein, J. Phys.: Condens. Matter **9**, 767 (1997); A.B. Shick, A.I. Liechtenstein, and W.E. Pickett, Phys. Rev. B **60**, 10 763 (1999).

[10] R. Weht and W.E. Pickett, Phys. Rev. Lett. **81**, 2502 (1998).

[11] V. Eyert, K.-H. Höch, and P.S. Riseborough, Europhys. Lett. **31**, 385 (1995).

[12] A. Collomb *et al.*, J. Magn. Magn. Mater. **7**, 1 (1978); Z. Zeng *et al.*, J. Solid State Chem. **147**, 185 (1999).

[13] B. Bochu *et al.*, J. Magn. Magn. Mater. **15-18**, 1319 (1980).

[14] C. Lacroix, J. Phys. C **13**, 5125 (1980).

[15] A. Collomb, D. Samaras, B. Bochu, and J.C. Joubert, Phys. Status Solidi A **41**, 459 (1977).

[16] W.E. Pickett and J.S. Moodera, Phys. Today **54** (5), 39 (2001).

[17] H.Y. Hwang and C.-W. Cheong, Science **278**, 1607 (1997).

[18] K.-I. Kobayashi *et al.*, Phys. Rev. B **59**, 11 159 (1999).